

***RMI1/NCE4*, a suppressor of genome instability, encodes a member of the RecQ helicase/Topo III complex**

**Michael Chang¹, Mohammed Bellaoui¹,
Chaoying Zhang¹, Ridhdi Desai¹, Pavel
Morozov², Lissette Delgado-Cruzata³,
Rodney Rothstein⁴, Greg A Freyer^{3,5},
Charles Boone⁶ and Grant W Brown^{1,*}**

¹Department of Biochemistry, University of Toronto, Toronto, Ontario, Canada, ²Columbia Genome Center, Columbia University, New York, NY, USA, ³Department of Environmental Health Sciences, Columbia University, New York, NY, USA, ⁴Department of Genetics and Development, Columbia University, New York, NY, USA, ⁵Department of Anatomy and Cell Biology, Columbia University, New York, NY, USA and ⁶Banting and Best Department of Medical Research and Department of Medical Genetics and Microbiology, University of Toronto, Toronto, Ontario, Canada

***SGS1* encodes a DNA helicase whose homologues in human cells include the *BLM*, *WRN*, and *RECQ4* genes, mutations in which lead to cancer-predisposition syndromes. Clustering of synthetic genetic interactions identified by large-scale genetic network analysis revealed that the genetic interaction profile of the gene *RMI1* (RecQ-mediated genome instability, also known as *NCE4* and *YPL024W*) was highly similar to that of *SGS1* and *TOP3*, suggesting a functional relationship between *Rmi1* and the *Sgs1/Top3* complex. We show that *Rmi1* physically interacts with *Sgs1* and *Top3* and is a third member of this complex. Cells lacking *RMI1* activate the *Rad53* checkpoint kinase, undergo a mitotic delay, and display increased relocalization of the recombination repair protein *Rad52*, indicating the presence of spontaneous DNA damage. Consistent with a role for *RMI1* in maintaining genome integrity, *rmi1Δ* cells exhibit increased recombination frequency and increased frequency of gross chromosomal rearrangements. In addition, *rmi1Δ* strains fail to fully activate *Rad53* upon exposure to DNA-damaging agents, suggesting that *Rmi1* is also an important part of the *Rad53*-dependent DNA damage response.**

The EMBO Journal (2005) 24, 2024–2033. doi:10.1038/sj.emboj.7600684; Published online 12 May 2005

Subject Categories: genome stability & dynamics

Keywords: checkpoint; genome instability; RecQ helicase; *Sgs1*; *Top3*

*Corresponding author. Department of Biochemistry, University of Toronto, 1 King's College Circle, Toronto, Ontario, Canada M5S 1A8. Tel.: +1 416 946 5733; Fax: +1 416 978 8548; E-mail: grant.brown@utoronto.ca

Received: 17 February 2005; accepted: 27 April 2005; published online: 12 May 2005

Introduction

Saccharomyces cerevisiae *SGS1* is a member of the *recQ* family of 3'–5' DNA helicases, which includes five human homologues (*RECQL*, *BLM*, *WRN*, *RECQ4*, and *RECQ5*) (Watt *et al*, 1995, 1996). Loss-of-function mutations in *BLM*, *WRN*, and *RECQ4* give rise to Bloom's syndrome (BS), Werner's syndrome (WS), and Rothmund–Thomson syndrome (RTS), respectively (Ellis *et al*, 1995; Yu *et al*, 1996; Kitao *et al*, 1999). Although the spectrum of clinical features of each disease differs, they all result in a predisposition to cancer. The major defects of cells with mutated *recQ* helicases are hyper-recombination and genomic instability (Hickson, 2003). *S. cerevisiae* *sgs1* mutants show elevated levels of mitotic homologous recombination, illegitimate recombination (Gangloff *et al*, 1994; Watt *et al*, 1996; Yamagata *et al*, 1998), sister chromatid exchanges (Onoda *et al*, 2000), and gross chromosomal rearrangements (GCRs) (Myung *et al*, 2001b; Myung and Kolodner, 2002). Cells lacking *SGS1* are also moderately sensitive to genotoxic agents such as methyl methanesulfonate (MMS) and hydroxyurea (HU) (Gangloff *et al*, 1994; Watt *et al*, 1996; Yamagata *et al*, 1998; Chang *et al*, 2002).

A subset of RecQ family members physically interacts with topoisomerase III (*Top3*) homologues (Gangloff *et al*, 1994; Goodwin *et al*, 1999; Johnson *et al*, 2000; Wu *et al*, 2000). *Escherichia coli* RecQ stimulates *Top3* to catenate and decatenate covalently closed duplex DNA (Harmon *et al*, 1999) and *BLM* is able to stimulate the DNA strand passage activity of *Top3α* (Oakley and Hickson, 2002). Furthermore, *BLM* and *Top3α* can work together to resolve a recombination intermediate containing a double Holliday junction (Wu and Hickson, 2003). *S. cerevisiae* strains lacking *TOP3* exhibit a severe growth defect, sensitivity to DNA-damaging agents, and hyper-recombination (Wallis *et al*, 1989; Gangloff *et al*, 1994; Chang *et al*, 2002). Most of the defects exhibited by *top3* mutants can be suppressed by mutation of *SGS1* (Gangloff *et al*, 1994; Chakraverty *et al*, 2001), a relationship that is conserved in *Schizosaccharomyces pombe* where mutations in the *recQ* homologue *rqh1*⁺ can suppress the lethality of *top3Δ* mutants (Maftahi *et al*, 1999). These data support models in which RecQ helicase action produces a toxic DNA structure that is resolved by *Top3* (Gangloff *et al*, 1994; Ira *et al*, 2003; Wu and Hickson, 2003).

Two-dimensional hierarchical clustering of synthetic genetic interactions determined by large-scale genetic network analysis in *S. cerevisiae* has proven useful for identifying genes whose products function within the same pathway or complex (Tong *et al*, 2004). Such clustering analysis revealed that the genetic interaction profile of the poorly characterized gene *RMI1* (RecQ-mediated genome instability) was highly similar to that of *SGS1* and *TOP3*. We show that *Rmi1* associates with *Sgs1* and *Top3* and that strains lacking

RMI1 accumulate DNA damage in the absence of exogenous genotoxic agents. Our results indicate that the actions of Sgs1, Top3, and Rmi1 are required in concert in order to maintain genome integrity.

Results

Mutations in *SGS1* can suppress the growth defects of an *rmi1Δ* mutant

Two-dimensional hierarchical clustering of large-scale synthetic genetic array (SGA) data revealed that the set of genes that genetically interact with the uncharacterized gene *RMI1* was highly similar to that associated with *SGS1*, *TOP3*, and *YLR235C* (which overlaps the *TOP3* open reading frame (ORF) such that a deletion of this ORF likely results in a *TOP3* hypomorph) (Tong *et al*, 2004; Supplementary Figure S1). Synthetic genetic interactions are usually orthogonal to protein–protein interactions, but the products of genes with similar patterns of genetic interactions are often found in the same cellular pathway or protein complex (Tong *et al*, 2004), suggesting that *RMI1* might function in the *SGS1/TOP3* pathway.

Crossing the *rmi1Δ* strain from the *Saccharomyces* gene deletion collection with a wild-type strain revealed the presence of an extragenic suppressor in the *rmi1Δ* strain. Tetrads from this cross were dissected to analyze the products of individual meioses (Figure 1A). The resultant colonies were screened to identify those carrying the *rmi1Δ* mutation. We

found that roughly half (10 of 24) of the *rmi1Δ* isolates exhibited a slow growth phenotype, whereas the other half (14 of 24) grew relatively normally, indicating that the original strain did indeed carry a single extragenic suppressor mutation. To identify the suppressor (*supX*), we employed synthetic genetic array mapping (SGAM) methodology, in which an *rmi1Δ supX* query strain was crossed to an array of ~4600 viable gene deletion mutants. This method maps a group of genes that are tightly linked to the suppressor (Jorgensen *et al*, 2002). Indeed, we identified a group of linked genes on chromosome XIII (Figure 1B), indicating that the suppressor was in this region. The *SGS1* gene was located in the middle of this linkage group, and the *sgs1Δ* strain was not identified in the SGAM experiment, suggesting that the suppressor might be a loss-of-function allele of *SGS1*. We crossed the *rmi1Δ* strain lacking the suppressor with an *sgs1Δ* strain and found that the double mutants had a normal growth phenotype (Figure 1C). We also sequenced the *SGS1* allele from the *rmi1Δ supX* strain and found that it carried a frame-shift mutation 691 nucleotides into the ORF and so encoded a truncated protein lacking the helicase catalytic domain of Sgs1. Therefore, deletion of *RMI1* causes a slow growth phenotype that can be suppressed by deletion of *SGS1*. This is reminiscent of the *TOP3* gene, deletion of which causes slow growth that is suppressed by mutation of *SGS1* (Wallis *et al*, 1989; Gangloff *et al*, 1994).

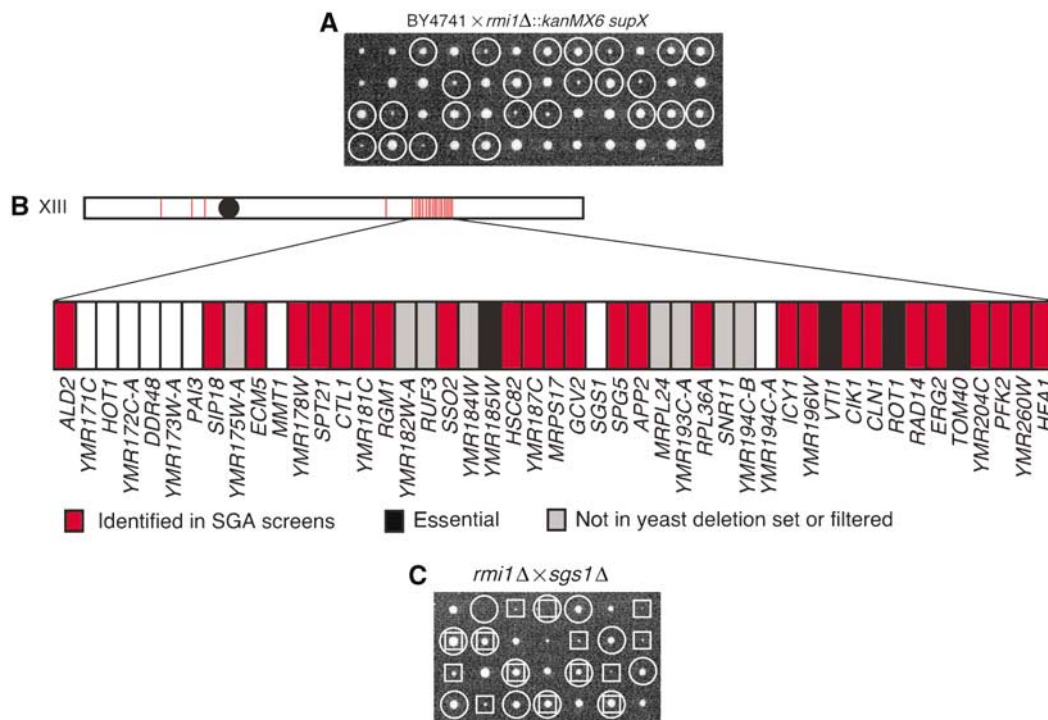


Figure 1 *rmi1Δ* mutants exhibit a growth defect that can be suppressed by mutation of *SGS1*. (A) The *rmi1Δ::kanMX6* strain was backcrossed to a wild-type strain (BY4741). The resulting diploids were sporulated and tetrads were dissected on YPD. Each column represents the four spores from a single tetrad. The genotypes of the resulting colonies are indicated with circles (○) for *rmi1Δ::kanMX6*. (B) SGAM analysis using an *rmi1Δ::natMX6* query strain (which contains *supX*) revealed a set of colinear synthetic genetic interactions on chromosome XIII. A red bar indicates that deletion of the corresponding gene resulted in a genetic interaction. Black bars represent essential genes, which are not a part of the gene deletion collection. Gray bars indicate ORFs for which no deletion mutant was made as part of the *Saccharomyces* Gene Deletion Project (Winzeler *et al*, 1999) and genes that are often found in control screens using a wild-type query strain, and therefore are filtered from the results of SGA analyses. (C) An *rmi1Δ::natMX6* strain lacking *supX* was crossed to an *sgs1Δ::kanMX6* strain. The resulting diploids were sporulated for tetrad analysis as in panel A. The genotypes of the resulting colonies are indicated with boxes (□) for *sgs1Δ::kanMX6* and circles (○) for *rmi1Δ::natMX6*.

Table I *rmi1Δ* genetic interactions

Gene	Interaction	Proposed function
<i>sgs1Δ</i>	Suppression	RecQ helicase
<i>top3Δ</i>	None	Type I topoisomerase
<i>rad53-11</i>	Lethality	DNA damage checkpoint
<i>mrc1Δ</i>	Sickness	S-phase DNA damage checkpoint
<i>csn3Δ</i>	Sickness	S-phase DNA damage checkpoint
<i>tof1Δ</i>	Sickness	S-phase DNA damage checkpoint
<i>rad9Δ</i>	None	G2 DNA damage checkpoint
<i>rad24Δ</i>	None	G2 DNA damage checkpoint
<i>rrm3Δ</i>	Lethality	DNA helicase; fork restart
<i>mus81Δ</i>	Lethality	Nuclease subunit; fork restart
<i>mms4Δ</i>	Lethality	Nuclease subunit; fork restart
<i>slx1Δ</i>	Lethality	Nuclease subunit; fork restart
<i>slx4Δ</i>	Lethality	Nuclease subunit; fork restart
<i>hex3Δ</i>	Lethality	Fork restart
<i>slx8Δ</i>	Lethality	Fork restart
<i>hpr5Δ</i>	Lethality	DNA helicase; fork restart
<i>rad51Δ</i>	Suppression	Homologous recombination
<i>rad52Δ</i>	Suppression	Homologous recombination
<i>rad54Δ</i>	Suppression	Homologous recombination

***rmi1Δ* synthetic genetic interactions**

Since the *rmi1Δ* mutant readily accumulates mutations in *SGS1*, we were unable to conduct an *RMI1* SGA analysis. Instead, we adopted a candidate approach, analyzing genes with connections to *SGS1* and *TOP3* function (Klein, 2001; Mullen *et al*, 2001; Tong *et al*, 2001, 2004) (Table I). We found that *rmi1Δ* is synthetic lethal when combined with mutations in genes thought to play roles in restarting stalled replication forks: *rrm3Δ*, *mus81Δ*, *mms4Δ*, *slx1Δ*, *slx4Δ*, *hex3Δ*, *slx8Δ*, and *hpr5Δ*. We also found that the slow growth phenotype of *rmi1Δ* was suppressed by *rad51Δ*, *rad52Δ*, and *rad54Δ*. This is consistent with models in which the presence of the homologous recombination pathway facilitates creation of DNA processing intermediates by Sgs1, which are toxic when Rmi1 is absent. Similar models have been proposed to account for the suppression of *top3Δ* phenotypes by mutations in recombination repair genes (Oakley *et al*, 2002; Shor *et al*, 2002). We also found that *rmi1Δ* did not display a detectable genetic interaction with *top3Δ*, consistent with *RMI1* and *TOP3* functioning in the same pathway. Finally, we found that homozygous *rmi1Δ/rmi1Δ* diploids are defective in undergoing meiosis to produce four spore asci (Supplementary Figure S2), indicating that like Sgs1 and Top3 (Watt *et al*, 1995; Gangloff *et al*, 1999), Rmi1 is essential for proper meiotic cell division.

Rmi1* physically interacts with *Top3* and *Sgs1

Genetic analysis placed *RMI1* in the *SGS1/TOP3* pathway and indicated in several ways that *rmi1Δ* phenocopies *top3Δ*. To gain insight into the mechanism underlying these genetic observations, we tested whether Rmi1 physically associates with Sgs1 and Top3. Sgs1 and Top3 interact *in vivo* and *in vitro* (Gangloff *et al*, 1994; Bennett *et al*, 2000; Fricke *et al*, 2001); however, the apparent molecular mass of Sgs1/Top3 complexes in yeast extracts suggests that the complexes are not heterodimeric and so may contain other proteins (Fricke *et al*, 2001). We used strains containing *SGS1*, *TOP3*, and *RMI1* epitope-tagged at their respective genomic loci to perform co-immunoprecipitations. Rmi1 was found in complex with both Sgs1 and Top3 (Figure 2A and B). This complex was not disrupted in the presence of DNase I,

indicating that the interactions are not mediated by DNA (Supplementary Figure S3). When Rmi1-TAP immunoprecipitations were quantified by densitometry, we found that 39% of Rmi1 was depleted from the extract compared with 42% of Sgs1 (data not shown), indicating that a significant fraction of Sgs1 is in complex with Rmi1. We next used gel filtration chromatography to fractionate extract from the tagged strain. We found that Sgs1-HA, Top3-VSV, and Rmi1-TAP co-elute in a high-molecular-weight complex (Figure 2C). Monomeric Rmi1 was not detected. Together, these data suggest that Rmi1 is in a heteromeric complex with both Sgs1 and Top3 and functions as a subunit of the Sgs1/Top3 complex.

Immunoprecipitates of Rmi1-TAP from extracts of an *sgs1Δ* strain contain Top3 (Figure 2B), indicating that the interaction of Rmi1 with Top3 does not require Sgs1. When attempting reciprocal experiments, we found that deletion of either *TOP3* or *RMI1* caused a significant reduction in Sgs1 protein abundance (data not shown). Despite the reduced levels of Sgs1, we detected Sgs1 in both Top3 immunoprecipitates from *rmi1Δ* cells and in Rmi1 immunoprecipitates from *top3Δ* cells (Figure 2D). Both wild-type and catalytically inactive helicase-dead mutant Sgs1 were poorly expressed in both *rmi1Δ* and *top3Δ* mutants (Figure 2E), indicating that the helicase activity of Sgs1 is not required for the observed reduction in Sgs1 levels.

***Cells lacking RMI1* display precocious checkpoint activation**

RecQ helicases are thought to play a role in normal DNA replication. The human homologues BLM and WRN are required for normal S-phase progression (Lonn *et al*, 1990; Poot *et al*, 1992). Completion of replication in the rDNA array is severely retarded in *sgs1Δ* mutants (Kaliraman and Brill, 2002; Versini *et al*, 2003), and *in vitro* replication in *Xenopus* egg extracts in the absence of Xblm results in DNA strand breaks (Li *et al*, 2004). We asked whether Rmi1 was also required for normal S-phase progression. Using cells released synchronously from a G1 arrest, we could not detect a significant defect in bulk DNA synthesis, as assessed by flow cytometry (Supplementary Figure S4). However, asynchronous *rmi1Δ* cultures exhibited an accumulation of budded cells with one nucleus, suggesting a delay in the late S/G2 phase of the cell cycle (Figure 3A). These observations are similar to those made with *top3Δ* strains (Gangloff *et al*, 1994; Chakraverty *et al*, 2001) and may indicate a checkpoint-dependent mitotic delay. We assayed for activation of the checkpoint kinase Rad53 in these cells, analyzing both the phosphorylation-dependent mobility shift of Rad53 and Rad53 kinase activity (Figure 3B and C). We found that *rmi1Δ* mutants displayed a modest mobility shift of Rad53 when released from a G1 arrest in the absence of any DNA-damaging agent (Figure 3B). This mobility shift is due to phosphorylation and correlates with activation of Rad53 kinase activity (Pelliccioli *et al*, 1999). We measured Rad53 activation directly using an *in situ* kinase assay. Activation of Rad53 in *rmi1Δ* was clearly evident in this assay, even in the sample from the asynchronous culture and from the G1-arrested culture (Figure 3C). Activation of Rad53 was not evident in wild-type cells in either assay. The precocious Rad53 checkpoint activation is likely the cause of the mitotic delay observed in *rmi1Δ*, suggesting that DNA damage is arising in cells lacking Rmi1 during an unperturbed cell cycle.

Consistent with this interpretation, we found that *rmi1Δ* is synthetic lethal with *rad53-11* (Figure 3D), a checkpoint defective allele of *RAD53* (Weinert *et al*, 1994), indicating that an intact checkpoint response is essential for the viability of cells lacking Rmi1.

We investigated the requirement for other checkpoint proteins in *rmi1Δ* mutants. We found that deletion of the G1 and G2 DNA damage checkpoint genes *RAD24* or *RAD9* had no detectable effect on the *rmi1Δ* mutant. However, deletion of the S-phase checkpoint genes *MRC1*, *TOF1*, or *CSM3* in the *rmi1Δ* mutant caused a synthetic sick phenotype

(Table I). Therefore, cells lacking *RMI1* require the S-phase checkpoint response for optimal growth, suggesting that the DNA damage caused by deletion of *RMI1* results from DNA replication defects.

rmi1Δ mutants exhibit increased levels of Rad52 relocalization and genomic instability

RAD52 is essential for efficient homologous recombination. Rad52 relocalizes from a diffuse nuclear localization to distinct subnuclear foci in response to DNA damage, particularly double-strand breaks (DSBs) (Lisby *et al*, 2001, 2003, 2004). Rad52 tagged with yellow fluorescent protein (Lisby *et al*, 2003, 2004) was visualized by fluorescence microscopy in asynchronous mitotic haploid cells. As shown in Figure 4A, cells lacking *RMI1* display subnuclear Rad52 foci, whereas wild-type cells show infrequent and transient foci. Quantification of the data (Figure 4B) showed that *rmi1Δ*, *sgs1Δ*, and *top3Δ* all have elevated levels of spontaneous Rad52 focus formation, indicating the presence of DNA damage requiring homologous recombination for repair, likely DSBs. Elevated levels of Rad52 foci were observed both in S/G2/M (i.e. budded) cells and in G1 cells. Together with the data indicating that Rad53 is activated in *rmi1Δ* mutants, these results suggest that DNA replication in the absence of an intact Sgs1/Top3/Rmi1 pathway causes DNA lesions that result in genomic instability (Gangloff *et al*, 1994; Myung *et al*, 2001b; Ajima *et al*, 2002), similar to the effect observed in *Xenopus* egg extracts, in which replication in the absence of Xblm causes DNA strand breaks (Li *et al*, 2004).

To assess the effect of the DNA damage that arises in *rmi1Δ* mutants, we applied two assays for genomic instability. Both *SGS1* and *TOP3* are suppressors of homologous recombination (Shor *et al*, 2002). We tested the effect of deletion of *RMI1* on homologous recombination using a *LEU2* direct repeat assay (Smith and Rothstein, 1999). Consistent with the observation that cells lacking *RMI1* have high levels of Rad52 foci, we found that *rmi1Δ* cells have an increased rate of recombination (Figure 5A), approximately six-fold higher than wild type. We also measured the rate of GCRs in *rmi1Δ*,

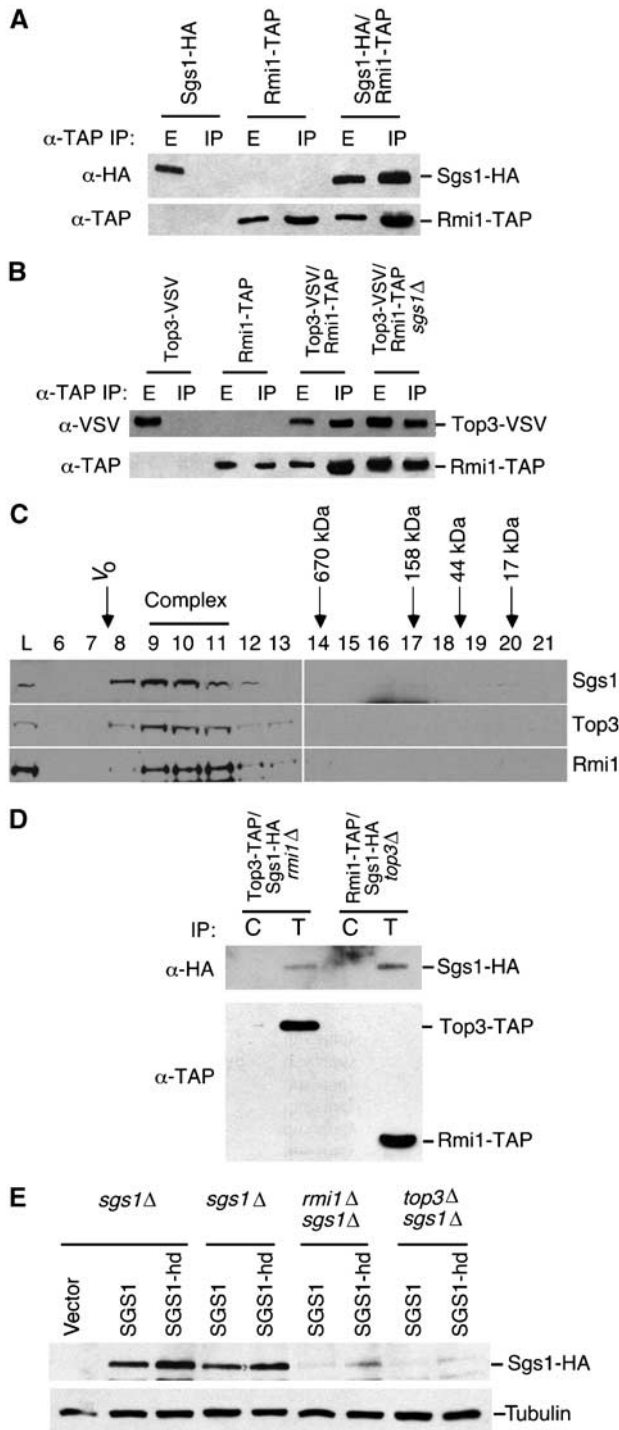


Figure 2 Rmi1 physically associates with the Sgs1/Top3 complex. (A, B) Extracts from yeast strains expressing the indicated epitope-tagged proteins were immunoprecipitated with IgG agarose. In all, 10% of the input extract (E) and the immunoprecipitate (IP) was fractionated by SDS-PAGE. Immunoblots were probed with anti-HA antibody to detect Sgs1, with anti-VSV antibody to detect Top3, or with peroxidase-anti-peroxidase to detect Rmi1-TAP. (C) Extract from a yeast strain expressing Sgs1-HA, Top3-VSV, and Rmi1-TAP was fractionated on a Superose 6 gel filtration column. Fractions were precipitated with TCA and analyzed by immunoblotting. The elution positions of molecular weight standards are indicated, as is the void volume of the column (V_0). (D) Extracts from yeast strains expressing Sgs1-HA and Top3-TAP or Sgs1-HA and Rmi1-TAP in an *rmi1Δ* or *top3Δ* background, respectively, were immunoprecipitated with IgG agarose to precipitate the TAP-tagged protein (lanes marked T) or with unconjugated agarose as a control (lanes marked C). The precipitates were immunoblotted and probed with anti-HA antibodies to detect Sgs1-HA (top panel) or with peroxidase-anti-peroxidase to detect the TAP-tagged proteins. (E) *sgs1Δ*, *sgs1Δ rmi1Δ*, and *sgs1Δ top3Δ* strains were transformed with empty vector (vector) or low-copy plasmids expressing HA-tagged Sgs1 (Sgs1) or helicase-dead Sgs1 (Sgs1-hd). TCA-fixed extracts were prepared and fractionated by SDS-PAGE. Immunoblots were probed with anti-HA antibody to detect Sgs1 or Sgs1-hd, and with anti-tubulin antibodies as a loading control.

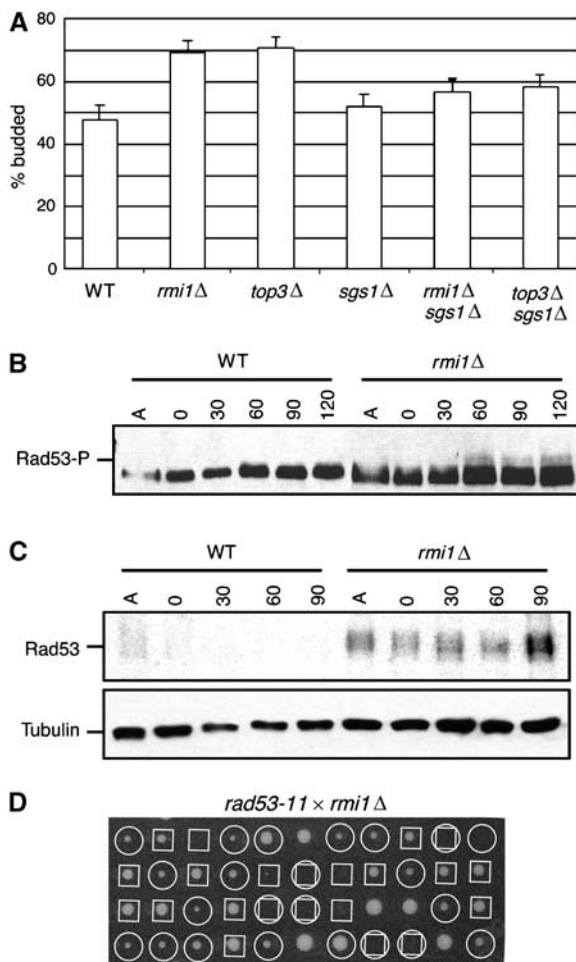


Figure 3 *rmi1*Δ mutants exhibit Rad53 checkpoint activation during an unperturbed cell cycle. (A) Asynchronous cultures of wild type (WT), *rmi1*Δ, *top3*Δ, *sgs1*Δ, *rmi1*Δ *sgs1*Δ, and *top3*Δ *sgs1*Δ were examined microscopically to determine the % of cells with a bud. (B) Logarithmically growing cultures were arrested in G1 with alpha factor and released into fresh YPD media. At the indicated times, samples were fixed with TCA, extracts were fractionated on SDS-PAGE, and immunoblotted to detect Rad53. The position of the activated phosphorylated Rad53 is indicated. (C) Samples prepared as in panel B were fractionated on SDS-PAGE for *in situ* kinase assay of Rad53 (upper panel). A parallel blot was probed with anti-tubulin antibody as a loading control (lower panel). (D) An *rmi1*Δ::*kanMX6* strain was crossed to a *rad53-11*::*URA3* strain. The resulting diploids were sporulated and tetrads were dissected on YPD. The genotypes of the resulting colonies are indicated with boxes (□) for *rmi1*Δ::*kanMX6* and with circles (○) for *rad53-11*::*URA3*. Inferred double mutants are indicated with a box and circle.

using an assay that detects large interstitial deletions, translocations, chromosome fusions, and loss of a chromosome arm (Myung *et al*, 2001a). In this assay (Figure 5B), *sgs1*Δ and *top3*Δ showed increased GCR rates of approximately 30-fold over wild type, similar to reported values (Myung *et al*, 2001b). In contrast, GCR rates in *rmi1*Δ were more than 150 times wild-type levels. Thus, Rmi1 is a critical suppressor of GCRs.

RMI1 is required for the response to DNA damage

Both *SGS1* and *TOP3* are important for the response to DNA damage (Stewart *et al*, 1997; Davey *et al*, 1998; Frei and

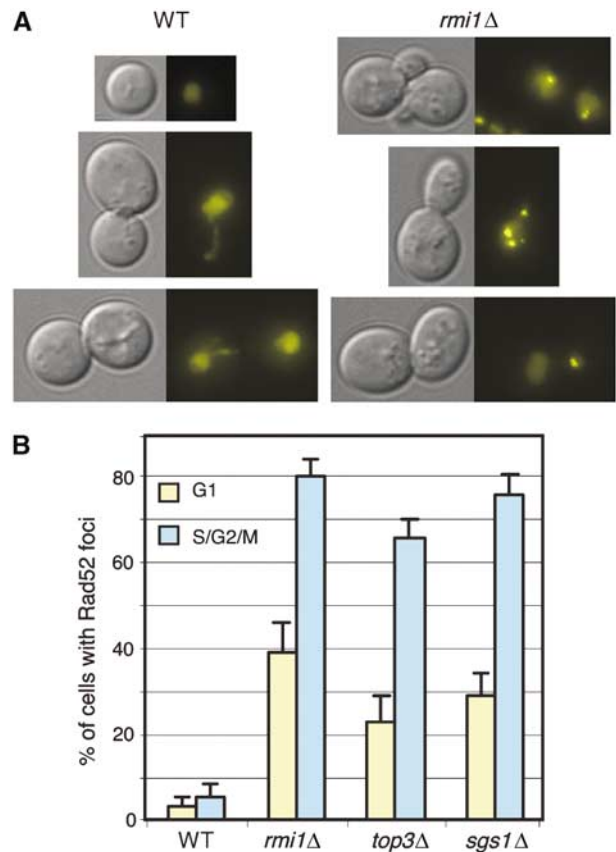


Figure 4 Spontaneous Rad52 focus formation in *rmi1*Δ cells. (A) Logarithmically growing cells expressing Rad52-YFP were visualized by fluorescence microscopy. For each pair of images, the left panel is a DIC image and the right panel is a fluorescence image showing Rad52-YFP. Representative cells are shown. (B) The percentage of cells with Rad52 foci was determined for the indicated strains. G1 cells with Rad52 foci are represented by the gold bars and S/G2/M cells with Rad52 foci are represented by the blue bars. WT, wild type.

Gasser, 2000; Chakraverty *et al*, 2001); therefore, we tested whether deletion of *RMI1* caused sensitivity to DNA-damaging agents (Figure 6A and B). The *rmi1*Δ, like *top3*Δ, displayed slow growth on YPD. The presence of the alkylating agent MMS (at 0.004%) or the replication inhibitor HU (at 10 mM) reduced colony formation by *rmi1*Δ by at least an order of magnitude, indicating that the *rmi1*Δ mutant is sensitive to DNA damage and replication stress. Wild-type cells were unaffected by the levels of MMS and HU used. We also tested whether *rmi1*Δ loses viability during transient exposure to the same concentrations of MMS or HU. The *rmi1*Δ mutant rapidly lost viability during exposure to MMS. During transient exposure to 10 mM HU, the *rmi1*Δ mutant displayed little loss of viability, although the growth of *rmi1*Δ was significantly impaired (Figure 6B). These results are reminiscent of *top3*Δ, which displays much greater sensitivity to transient MMS exposure than it does to transient HU exposure (Chakraverty *et al*, 2001; Oakley *et al*, 2002). The DNA damage sensitivity and loss of viability of *rmi1*Δ were suppressed by deletion of *SGS1*, with the double mutant displaying growth similar to that of *sgs1*Δ.

Top3 is important for full activation of Rad53 in response to DNA damage (Chakraverty *et al*, 2001) while Sgs1 is

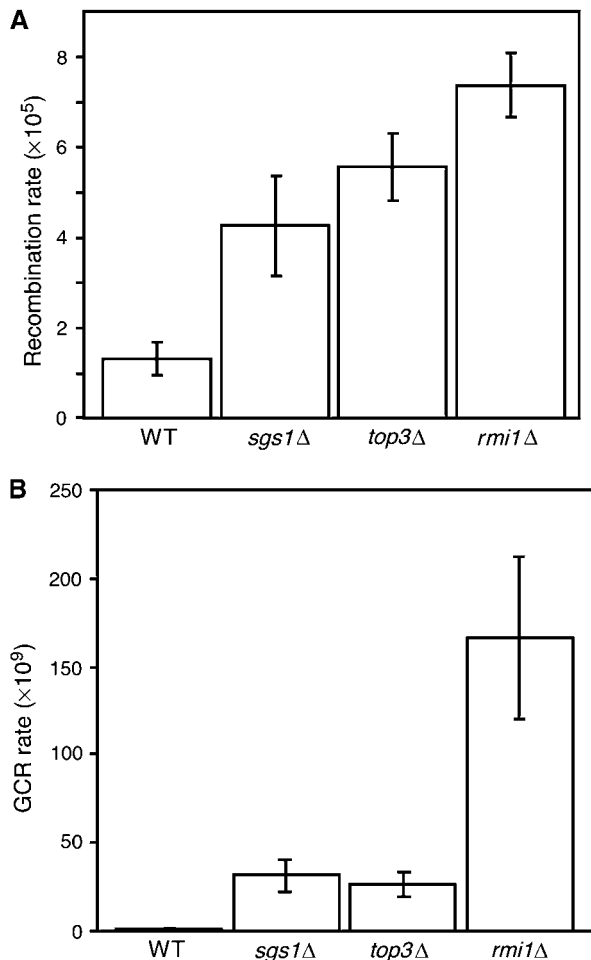


Figure 5 Deletion of *RMI1* causes genomic instability. (A) Recombination rate was measured using a direct repeat recombination assay. The average and standard deviation of three fluctuation tests are shown for each strain. (B) GCR rate was measured. The average and standard deviation of four fluctuation tests are shown for each strain. WT, wild type.

necessary for Rad53 activation in the absence of Rad24 (Frei and Gasser, 2000; Bjergbaek *et al*, 2005). We tested whether *RMI1* was also important for Rad53 activation. Rad53 activation was measured after treatment with HU or MMS (Figure 6C). Wild-type cells showed a robust checkpoint response, resulting in phosphorylation-dependent mobility shift of Rad53. By contrast, *rmi1* Δ mutants showed a defect in Rad53 activation in response to both HU and MMS, as evidenced by incomplete phosphorylation of Rad53. This defect can be suppressed by mutation of *SGS1* (data not shown), similar to the suppression of the Rad53 activation defect in a *top3* Δ mutant by deletion of *SGS1* (Chakraverty *et al*, 2001). Thus, in addition to causing DNA damage during S phase, deletion of *RMI1* impedes full checkpoint activation when cells are challenged with exogenous damaging agents, suggesting that like Sgs1 and Top3, Rmi1 is upstream of Rad53 in the S-phase checkpoint response.

Evolutionary conservation of Rmi1

Homologues of Sgs1 and Top3 are found throughout Eucaryota. Using local alignment searches, we identified homologues of Rmi1 in six other yeast species. Sequence

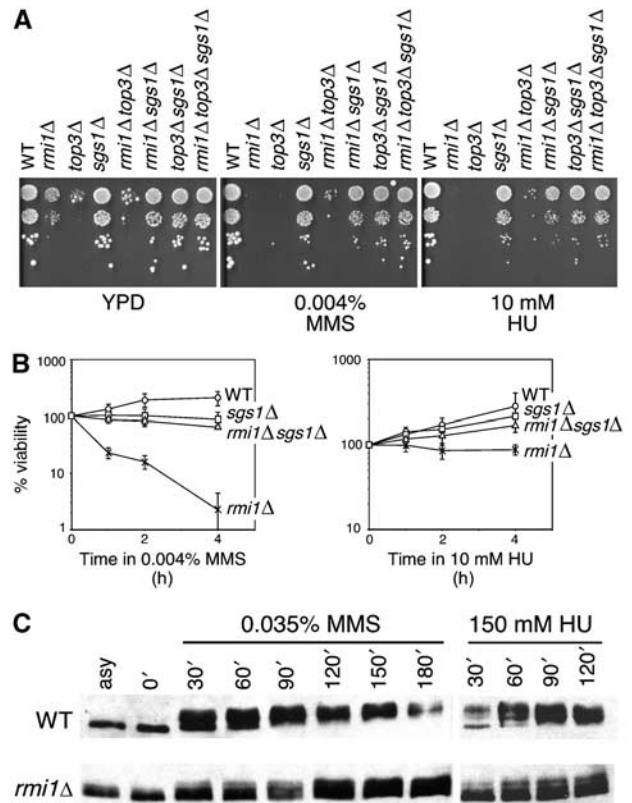


Figure 6 Rmi1 is required for the DNA damage response. (A) Serial dilutions (10-fold) of cultures of the indicated mutants were spotted on YPD, YPD containing 0.004% (v/v) MMS, or YPD containing 10 mM HU. All plates were incubated at 30°C for 2–3 days. (B) Logarithmically growing cultures of the indicated mutants were incubated in YPD containing 0.004% (v/v) MMS or 10 mM HU at 30°C. At the indicated times, samples were withdrawn and plated on YPD to determine the number of viable cells. The percentage of viable cells relative to the number of viable cells at $t = 0$ is shown. Plots represent the average of three experiments, and error bars span 1 s.d. (C) Logarithmically growing cultures were arrested in G1 with alpha factor and released into medium containing either 0.035% (v/v) MMS or 150 mM HU. At the indicated times, samples were fixed and extracts fractionated by SDS-PAGE. Following transfer, the immunoblot was probed with anti-Rad53 antibody. WT, wild type.

alignments of yeast Rmi1 homologues indicated that these proteins share three blocks of high sequence similarity (Figure 7A and Supplementary Figure S5).

In fission yeast, the *top3*⁺ gene is essential for viability (Goodwin *et al*, 1999; Maftahi *et al*, 1999), a phenotype that is suppressed by deletion of the fission yeast RecQ homologue *rql1*⁺ (Goodwin *et al*, 1999; Maftahi *et al*, 1999). We asked whether the fission yeast *rmi1*⁺ gene is, like *top3*⁺, essential for viability by replacing the *rmi1*⁺ ORF with a G418 resistance gene in a haploid strain carrying a deletion of the *rql1*⁺ gene (*rql1* Δ ::*ura4*⁺). This strain was viable, indicating that *rmi1*⁺ is not essential in an *rql1* Δ background. The *rmi1* Δ ::*G418*^R *rql1* Δ ::*ura4*⁺ strain was crossed to a wild-type strain and meiotic progeny were examined following tetrad dissection (Figure 7B). All inferred *rmi1* Δ single mutants failed to form colonies, indicating that *rmi1*⁺ is an essential gene. Examination of the resulting microcolonies revealed that the *rmi1* Δ cells go through several divisions before arresting with an elongated morphology (Figure 7C), a

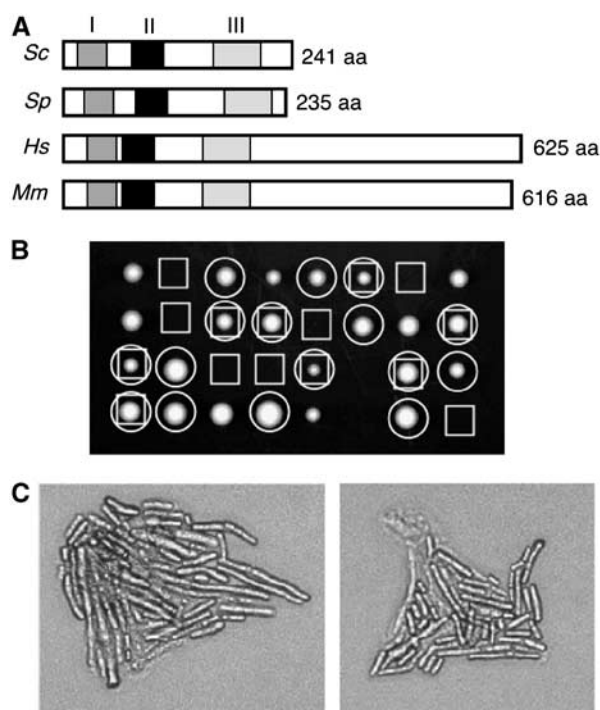


Figure 7 Rmi1 homologues. (A) Schematic diagrams of Rmi1 homologues from *S. cerevisiae* (Sc), *S. pombe* (Sp), *Homo sapiens* (Hs), and *Mus musculus* (Mm). Regions of high sequence identity are indicated by the three shaded boxes. (B) *S. pombe* *rmi1*⁺ is a functional homologue of *RM11*. *rmi1Δ::G418^R rqh1Δ::ura4⁺* was crossed to *rmi1⁺ rqh1⁺* and tetrads were dissected on YE5S. The genotypes of the resulting colonies are indicated with boxes (□) for (inferred) *rmi1Δ::G418^R* and with circles (○) for *rqh1Δ::ura4⁺*. (C) Micrographs of *rmi1Δ::G418^R rqh1Δ::ura4⁺* microcolonies from panel C.

phenotype similar to that found with *top3Δ* mutants (Maftahi *et al*, 1999). These results suggest that the fission yeast *rmi1*⁺ is the functional homologue of budding yeast *RM11*.

We extended our homology search to metazoan species and found that homologues were not readily identified using local alignment searches such as BLAST. We used the three regions of sequence similarity from the yeast analysis to build a hidden Markov model (HMM) for each region. The HMMs were then used to search the NCBI nonredundant protein database, resulting in the identification of homologous proteins in humans and mice. These putative Rmi1 homologues contain the three conserved regions that were evident in the yeast homologues, and also contain a C-terminal extension (Figure 7A and Supplementary Figure S6). The human Rmi1 homologue is identical to the recently described BLAP75, a BLM-associated protein that is important for genome integrity in human cells (Yin *et al*, 2005).

Discussion

Rmi1 is a novel member of the Sgs1/Top3 complex

We have found that Rmi1 physically associates with both Sgs1 and Top3. Fractionation of cell extracts by gel filtration chromatography and co-immunoprecipitation experiments indicated that Rmi1 is in a high-molecular-weight heteromeric complex that contains both Sgs1 and Top3. In the absence of Rmi1, the levels of Sgs1 decrease, an effect that

is also observed in the absence of the Sgs1 binding partner Top3. This suggests that interactions with both Rmi1 and Top3 are important for Sgs1 stability. Finally, *rmi1Δ* shares many phenotypes with *top3Δ*, including slow growth and DNA damage sensitivities that are suppressed by deletion of *SGS1*, indicating that Rmi1 is required for Top3 function *in vivo* (or *vice versa*). The simplest interpretation of these data is that Rmi1 is a member of the functional Sgs1/Top3 complex. The exact stoichiometry and architecture of the native cellular Sgs1/Top3/Rmi1 complex remains elusive as Sgs1 is present in a very high-molecular-weight complex of some 1.3 MDa (Fricke *et al*, 2001), suggesting that other proteins may also be present. Thus, the interaction of Rmi1 with Sgs1/Top3 may be direct or indirect.

The reduction of Sgs1 steady-state protein levels in an *rmi1Δ* or *top3Δ* background is especially intriguing given that deleting *SGS1* in these backgrounds improves cell viability. Therefore, it appears that even a very low level of Sgs1 is detrimental to cells lacking Rmi1 or Top3. Although abolishing the helicase activity of Sgs1 improves viability of *rmi1Δ* (data not shown) and *top3Δ* mutants (Mullen *et al*, 2001), levels of helicase-dead Sgs1 were still greatly reduced in *rmi1Δ* and *top3Δ* compared to wild type (Figure 2E), indicating that the reduced Sgs1 levels are unlikely to be a response to Sgs1 activity. The mechanism by which Sgs1 levels are reduced is currently unknown, but the phenomenon appears to be evolutionarily conserved in that deletion of *top3⁺* in *S. pombe* results in a reduction in the level of a helicase-inactive Rqh1 (Laursen *et al*, 2003). Although several models are consistent with our data, the simplest explanation is that absence of either Rmi1 or Top3 from the Sgs1/Top3/Rmi1 complex destabilizes Sgs1 but enough Sgs1 activity remains to cause reduced viability of *rmi1Δ* or *top3Δ* cells.

In vitro experiments using purified BLM and TOP3 α have demonstrated that together these proteins can resolve a recombination intermediate containing a double Holliday junction (Wu and Hickson, 2003). Deletion of *RM11* results in a phenotype very similar to that displayed by *top3Δ* mutants, suggesting that Rmi1 may be important for the biochemical activity of Top3. However, deletion of either *TOP3* or *RM11* causes a reduction in Sgs1 levels and so is likely to also compromise Sgs1 activity. Additionally, Rmi1 binds to both Top3 and Sgs1, further indicating that Rmi1 may influence the activity of both complex members. It will be of considerable interest to determine if and how the presence of Rmi1 affects the biochemical properties of RecQ/Top3 complexes.

Accumulation of DNA damage in cells lacking RM11

The mitotic cell cycle delay, precocious Rad53 activation, and synthetic genetic interactions with genes required for DNA replication fork stability and the S-phase checkpoint all point to the accumulation of DNA lesions. The genetic suppression data suggest that these lesions are generated from the processing of recombination intermediates by Sgs1. The exact nature of these lesions has yet to be determined but the elevated levels of GCRs, Rad52 foci, and recombination provide insight as to what these lesions may be. GCRs can take the form of nonreciprocal translocations, interstitial deletions, chromosome fusions, and loss of a chromosome arm followed by *de novo* telomere addition (Chen *et al*, 1998; Myung *et al*, 2001a). All of these rearrangements require the

creation of DSBs. Thus, we know that at least a significant fraction of the lesions generated in an *rmi1Δ* mutant are, or result in, DSBs. Consistent with this hypothesis, Rad52 relocalizes into DSB repair foci in *rmi1Δ*, presumably reflecting the observed increase in recombination frequency. Recent work indicates that abnormal recombination structures accumulate in *sgs1Δ* and *top3Δ* mutants when alkylation damage is present (Liberi *et al*, 2005). Accumulation of these structures was not detected in the absence of DNA damage, however. We found increased levels of Rad52 recombination repair foci in cells lacking Rmi1, Sgs1, or Top3 in an otherwise unperturbed cell cycle, which argues that Sgs1/Top3/Rmi1 function is required to prevent DNA damage from occurring during normal cell cycle progression. Interestingly, we found that the direct repeat recombination rate is higher in an *rmi1Δ* mutant than in an *sgs1Δ* mutant; yet, Rad52 foci form to the same extent in both. It has been shown that multiple DSBs can localize to one Rad52 focus; thus, the formation of Rad52 foci may not be directly proportional to the extent of DNA damage (Lisby *et al*, 2003). As suggested by their slower growth rate and precocious checkpoint activation, it is likely that *rmi1Δ* mutants accumulate more damage than *sgs1Δ* mutants, resulting in the higher rate of recombination observed. Alternatively, the DNA lesions present in *rmi1Δ* cells may simply be more recombinogenic than those present in *sgs1Δ* cells.

Defects in Rad53 checkpoint activation

Similar to *top3Δ* mutants (Chakraverty *et al*, 2001), cells lacking *RMI1* are defective in fully activating Rad53 in response to DNA damage induced by HU or MMS, a defect that can be suppressed by the mutation of *SGS1*. The Sgs1/Top3/Rmi1 complex may be needed to process DNA lesions in order to generate DNA structures that can be recognized by the DNA damage checkpoint machinery, allowing for checkpoint activation. Sgs1 function in the absence of Rmi1 or Top3 could generate a toxic DNA intermediate that is not efficiently recognized by the checkpoint machinery. Alternatively, Rmi1 could be required in a more direct way to facilitate Rad53 activation, perhaps by mediating localization of Rad53 to DNA lesions or stalled replication forks. Either model is consistent with the weak Rad53 activation seen in the Rad53 protein blots of extracts from *rmi1Δ* mutants treated with MMS or HU (Figure 6A). Although the failure of *rmi1Δ* mutants to support wild-type checkpoint activation may seem at odds with our data demonstrating precocious checkpoint activation in *rmi1Δ* in the absence of DNA-damaging agents, it is worth noting that Rad53 is in fact activated in *rmi1Δ* in response to MMS or HU, but to lower levels than in wild-type cells. Thus, the spontaneous damage present in *rmi1Δ* might cause more robust checkpoint activation if *rmi1Δ* mutants were not compromised in checkpoint activation. In this regard, it is interesting that we see evidence of spontaneous DNA damage in G1 *rmi1Δ* cells (Figure 4B). In wild-type cells, DNA damage accrued during G1 does not induce Rad52 foci formation until cells progress into S phase (Lisby *et al*, 2004). The presence of Rad52 foci in *rmi1Δ* G1 cells is likely due to progression through mitosis despite the presence of DNA lesions. Although a single DSB is typically sufficient to prevent passage through mitosis for several cell cycles (Lee *et al*, 1998), we would expect this checkpoint-mediated mitotic delay to be abrogated in mutants such as

rmi1Δ that display compromised checkpoint activation in response to DNA damage. Progression through mitosis in the presence of DNA lesions could be a principal cause of the poor viability of *rmi1Δ* mutants.

Recent data suggest that *top3Δ* mutants appear to have a compromised checkpoint due to impaired progression into and through S phase (Bjergbaek *et al*, 2005). A *rad24Δ top3Δ* double mutant, which does not exhibit these S-phase defects or the slow growth exhibited by a *top3Δ* mutant, is fully competent in activating Rad53 upon exposure to HU (Bjergbaek *et al*, 2005). Flow cytometric analysis of *rmi1Δ* mutants failed to detect a significant delay in progression into and through S phase, and we found that deletion of *RAD24* does not suppress the growth defect of an *rmi1Δ* mutant. Thus, the underlying mechanism by which the checkpoint is compromised in *rmi1Δ* may differ from that in *top3Δ*. Indeed, there are several aspects of the *rmi1Δ* phenotype that are different from that of *top3Δ*. *rmi1Δ* mutants grow slightly better than *top3Δ* mutants and there is a large difference in their GCR rates. These phenotypic differences are not surprising, given that loss of Top3 from the Rmi1/Sgs1/Top3 complex is likely to be biochemically distinct from loss of Rmi1.

RMI1 function in higher eukaryotes

We have identified homologues of budding yeast Rmi1 in several yeast species, as well as mouse and human. The presence of three conserved regions in diverse species suggests that these regions may constitute functional domains. Human Rmi1 has similarity to nucleic acid binding OB-folds (Koonin *et al*, 2000) extending through conserved regions II and III, raising the possibility that Rmi1 might bind DNA directly. Of particular interest, the putative human Rmi1 homologue that we identified by sequence similarity is identical to the recently described BLAP75 (Yin *et al*, 2005). Like Rmi1 in yeast, BLAP75 is an integral component of RecQ/Topo III complexes in human cells, and depletion of BLAP75 results in genome instability in the form of increased sister chromatid exchanges (Yin *et al*, 2005). Thus, the role of Rmi1 in RecQ/Top3 function appears to be conserved in all eukaryotes. Budding yeast Rmi1 is an important suppressor of DNA damage during S phase, and is also required for a robust checkpoint response to DNA damage and replication stress. It will be of great interest to determine if these functions are conserved in hRmi1/BLAP75, and if hRMI1/BLAP75 polymorphisms are associated with human cancers.

Materials and methods

Yeast strains and media

Yeast strains used in this study are derivatives of BY4741 (Brachmann *et al*, 1998) and are listed in Supplementary Table S1. Nonessential haploid deletion strains were made by the *Saccharomyces* Gene Deletion Project (Winzeler *et al*, 1999). Standard yeast media and growth conditions were used (Moreno *et al*, 1991; Sherman, 1991). For cell synchrony experiments, cells were arrested in G1 by culturing in the presence of 2 μg/ml alpha mating factor for 2 h at 30°C in YPD, pH 3.9. Cells were released into the cell cycle by harvesting, washing, and resuspending in YPD.

SGAM analysis

SGAM analysis was carried out as described (Tong *et al*, 2001, 2004; Jorgensen *et al*, 2002) to map the location of the extragenic suppressor in the *rmi1Δ::natR* query strain (Y5646).

Epitope tagging, immunoprecipitation, immunoblotting, and gel filtration

Immunoprecipitation was performed essentially as described (Bellaoui *et al*, 2003). Purified rabbit IgG agarose (Sigma) was used to immunoprecipitate TAP-tagged proteins, and immunoprecipitates were washed extensively with buffer containing 100 mM NaCl. Proteins were resolved on 7.5% polyacrylamide–SDS gels, transferred to nitrocellulose membranes, and subjected to immunoblot analysis with anti-HA (16B12; Covance), anti-VSV (P5D4; Roche), anti-tubulin (TAT-1) (Woods *et al*, 1989), or anti-TAP (PAP: peroxidase–anti-peroxidase soluble complex; Sigma) antibodies. Immunoblots were developed using Supersignal ECL (Pierce). For detection of Rad53 and *in situ* autophosphorylation assays, cells were fixed and extracts were prepared essentially as described (Pelliccioli *et al*, 1999). Proteins were separated on 7.5% polyacrylamide–SDS gels, and immunoblots were probed with anti-RAD53 (yC-19; Santa Cruz). Gel filtration of extracts of GY635 was carried out on a Superose 6 HR 5/20 column, essentially as described (Fricke *et al*, 2001).

Fluorescence microscopy

Cells containing the plasmid pWJ1344, which expresses Rad52-YFP, were grown to logarithmic phase at 23°C in SC medium lacking leucine. Microscopy was performed essentially as described (Lisby *et al*, 2001, 2003, 2004).

Recombination and GCR assays

Recombination assays were performed using a *LEU2* direct repeat, as described (Bellaoui *et al*, 2003). Fluctuation tests of five colonies

were repeated three times. GCR assays were performed as described (Myung *et al*, 2001a). Fluctuation tests of three colonies were repeated at least four times.

MMS and HU sensitivity measurements

Cells were grown in YPD, serially diluted, spotted onto plates, and incubated at 30°C. MMS (Aldrich) plates contained 0.004% (v/v) MMS in YPD and were used within 24 h of preparation. HU plates contained 10 mM HU in YPD. Viability following exposure to 0.004% MMS or 10 mM HU in liquid culture was determined as described (Bellaoui *et al*, 2003).

Supplementary data

Supplementary data are available at *The EMBO Journal* Online.

Acknowledgements

We thank Steve Brill for communicating results prior to publication, Igor Stagljar and Steve Brill for strains and plasmids, Dave Alvaro, Jackie Barlow, and Rebecca Burgess for assistance with Rad52 relocalization experiments, and Dan Durocher for constructive comments on the manuscript. MC was supported by an Ontario Graduate Scholarship. This work was supported by the Canadian Institutes of Health Research (to GWB and CB), Genome Canada and Genome Ontario (to CB), and the National Institutes of Health (CA072647 to GAF and GM50237 to RR). GWB is a Research Scientist of the National Cancer Institute of Canada.

References

- Ajima J, Umezu K, Maki H (2002) Elevated incidence of loss of heterozygosity (LOH) in an *sgs1* mutant of *Saccharomyces cerevisiae*: roles of yeast RecQ helicase in suppression of aneuploidy, interchromosomal rearrangement, and the simultaneous incidence of both events during mitotic growth. *Mutat Res* **504**: 157–172
- Bellaoui M, Chang M, Ou J, Xu H, Boone C, Brown GW (2003) Elg1 forms an alternative RFC complex important for DNA replication and genome integrity. *EMBO J* **22**: 4304–4313
- Bennett RJ, Noirot-Gros MF, Wang JC (2000) Interaction between yeast *sgs1* helicase and DNA topoisomerase III. *J Biol Chem* **275**: 26898–26905
- Bjergbaek L, Cobb JA, Tsai-Pflugfelder M, Gasser SM (2005) Mechanistically distinct roles for Sgs1p in checkpoint activation and replication fork maintenance. *EMBO J* **24**: 405–417
- Brachmann CB, Davies A, Cost GJ, Caputo E, Li J, Hieter P, Boeke JD (1998) Designer deletion strains derived from *Saccharomyces cerevisiae* S288C: a useful set of strains and plasmids for PCR-mediated gene disruption and other applications. *Yeast* **14**: 115–132
- Chakraverty RK, Kearsey JM, Oakley TJ, Grenon M, de La Torre Ruiz MA, Lowndes NF, Hickson ID (2001) Topoisomerase III acts upstream of Rad53p in the S-phase DNA damage checkpoint. *Mol Cell Biol* **21**: 7150–7162
- Chang M, Bellaoui M, Boone C, Brown GW (2002) A genome-wide screen for methyl methanesulfonate-sensitive mutants reveals genes required for S phase progression in the presence of DNA damage. *Proc Natl Acad Sci USA* **99**: 16934–16939
- Chen C, Umezu K, Kolodner RD (1998) Chromosomal rearrangements occur in *S. cerevisiae* *rfa1* mutator mutants due to mutagenic lesions processed by double-strand-break repair. *Mol Cell* **2**: 9–22
- Davey S, Han CS, Ramer SA, Klassen JC, Jacobson A, Eisenberger A, Hopkins KM, Lieberman HB, Freyer GA (1998) Fission yeast *rad12+* regulates cell cycle checkpoint control and is homologous to the Bloom's syndrome disease gene. *Mol Cell Biol* **18**: 2721–2728
- Ellis NA, Groden J, Ye TZ, Straughen J, Lennon DJ, Ciccio S, Proytcheva M, German J (1995) The Bloom's syndrome gene product is homologous to RecQ helicases. *Cell* **83**: 655–666
- Frei C, Gasser SM (2000) The yeast Sgs1p helicase acts upstream of Rad53p in the DNA replication checkpoint and colocalizes with Rad53p in S-phase-specific foci. *Genes Dev* **14**: 81–96
- Fricke WM, Kaliraman V, Brill SJ (2001) Mapping the DNA topoisomerase III binding domain of the Sgs1 DNA helicase. *J Biol Chem* **276**: 8848–8855
- Gangloff S, de Massy B, Arthur L, Rothstein R, Fabre F (1999) The essential role of yeast topoisomerase III in meiosis depends on recombination. *EMBO J* **18**: 1701–1711
- Gangloff S, McDonald JP, Bendixen C, Arthur L, Rothstein R (1994) The yeast type I topoisomerase Top3 interacts with Sgs1, a DNA helicase homolog: a potential eukaryotic reverse gyrase. *Mol Cell Biol* **14**: 8391–8398
- Goodwin A, Wang SW, Toda T, Norbury C, Hickson ID (1999) Topoisomerase III is essential for accurate nuclear division in *Schizosaccharomyces pombe*. *Nucleic Acids Res* **27**: 4050–4058
- Harmon FG, DiGate RJ, Kowalczykowski SC (1999) RecQ helicase and topoisomerase III comprise a novel DNA strand passage function: a conserved mechanism for control of DNA recombination. *Mol Cell* **3**: 611–620
- Hickson ID (2003) RecQ helicases: caretakers of the genome. *Nat Rev Cancer* **3**: 169–178
- Ira G, Malkova A, Liberi G, Foiani M, Haber JE (2003) Srs2 and Sgs1–Top3 suppress crossovers during double-strand break repair in yeast. *Cell* **115**: 401–411
- Johnson FB, Lombard DB, Neff NF, Mastrangelo MA, Dewolf W, Ellis NA, Marciniak RA, Yin Y, Jaenisch R, Guarente L (2000) Association of the Bloom syndrome protein with topoisomerase IIIalpha in somatic and meiotic cells. *Cancer Res* **60**: 1162–1167
- Jorgensen P, Nelson B, Robinson MD, Chen Y, Andrews B, Tyers M, Boone C (2002) High-resolution genetic mapping with ordered arrays of *Saccharomyces cerevisiae* deletion mutants. *Genetics* **162**: 1091–1099
- Kaliraman V, Brill SJ (2002) Role of SGS1 and SLX4 in maintaining rDNA structure in *Saccharomyces cerevisiae*. *Curr Genet* **41**: 389–400
- Kitao S, Lindor NM, Shiratori M, Furuichi Y, Shimamoto A (1999) Rothmund–Thomson syndrome responsible gene, RECQL4: genomic structure and products. *Genomics* **61**: 268–276
- Klein HL (2001) Mutations in recombinational repair and in checkpoint control genes suppress the lethal combination of *srs2Delta* with other DNA repair genes in *Saccharomyces cerevisiae*. *Genetics* **157**: 557–565
- Koonin EV, Wolf YI, Aravind L (2000) Protein fold recognition using sequence profiles and its application in structural genomics. *Adv Protein Chem* **54**: 245–275

- Laursen LV, Ampatzidou E, Andersen AH, Murray JM (2003) Role for the fission yeast RecQ helicase in DNA repair in G2. *Mol Cell Biol* **23**: 3692–3705
- Lee SE, Moore JK, Holmes A, Umez K, Kolodner RD, Haber JE (1998) *Saccharomyces* Ku70, mre11/rad50 and RPA proteins regulate adaptation to G2/M arrest after DNA damage. *Cell* **94**: 399–409
- Li W, Kim SM, Lee J, Dunphy WG (2004) Absence of BLM leads to accumulation of chromosomal DNA breaks during both unperturbed and disrupted S phases. *J Cell Biol* **165**: 801–812
- Liberi G, Maffioletti G, Lucca C, Chiolo I, Baryshnikova A, Cotta-Ramusino C, Lopes M, Pelliccioli A, Haber JE, Foiani M (2005) Rad51-dependent DNA structures accumulate at damaged replication forks in sgs1 mutants defective in the yeast ortholog of BLM RecQ helicase. *Genes Dev* **19**: 339–350
- Lisby M, Barlow JH, Burgess RC, Rothstein R (2004) Choreography of the DNA damage response: spatiotemporal relationships among checkpoint and repair proteins. *Cell* **118**: 699–713
- Lisby M, Mortensen UH, Rothstein R (2003) Colocalization of multiple DNA double-strand breaks at a single Rad52 repair centre. *Nat Cell Biol* **5**: 572–577
- Lisby M, Rothstein R, Mortensen UH (2001) Rad52 forms DNA repair and recombination centers during S phase. *Proc Natl Acad Sci USA* **98**: 8276–8282
- Lonn U, Lonn S, Nylén U, Winblad G, German J (1990) An abnormal profile of DNA replication intermediates in Bloom's syndrome. *Cancer Res* **50**: 3141–3145
- Maftahi M, Han CS, Langston LD, Hope JC, Zigouras N, Freyer GA (1999) The top3(+) gene is essential in *Schizosaccharomyces pombe* and the lethality associated with its loss is caused by Rad12 helicase activity. *Nucleic Acids Res* **27**: 4715–4724
- Moreno S, Klar A, Nurse P (1991) Molecular genetic analysis of fission yeast *Schizosaccharomyces pombe*. *Methods Enzymol* **194**: 795–823
- Mullen JR, Kaliraman V, Ibrahim SS, Brill SJ (2001) Requirement for three novel protein complexes in the absence of the Sgs1 DNA helicase in *Saccharomyces cerevisiae*. *Genetics* **157**: 103–118
- Myung K, Chen C, Kolodner RD (2001a) Multiple pathways cooperate in the suppression of genome instability in *Saccharomyces cerevisiae*. *Nature* **411**: 1073–1076
- Myung K, Datta A, Chen C, Kolodner RD (2001b) SGS1, the *Saccharomyces cerevisiae* homologue of BLM and WRN, suppresses genome instability and homeologous recombination. *Nat Genet* **27**: 113–116
- Myung K, Kolodner RD (2002) Suppression of genome instability by redundant S-phase checkpoint pathways in *Saccharomyces cerevisiae*. *Proc Natl Acad Sci USA* **99**: 4500–4507
- Oakley TJ, Goodwin A, Chakraverty RK, Hickson ID (2002) Inactivation of homologous recombination suppresses defects in topoisomerase III-deficient mutants. *DNA Repair (Amst)* **1**: 463–482
- Oakley TJ, Hickson ID (2002) Defending genome integrity during S-phase: putative roles for RecQ helicases and topoisomerase III. *DNA Repair (Amst)* **1**: 175–207
- Onoda F, Seki M, Miyajima A, Enomoto T (2000) Elevation of sister chromatid exchange in *Saccharomyces cerevisiae* sgs1 disruptants and the relevance of the disruptants as a system to evaluate mutations in Bloom's syndrome gene. *Mutat Res* **459**: 203–209
- Pelliccioli A, Lucca C, Liberi G, Marini F, Lopes M, Plevani P, Romano A, Di Fiore PP, Foiani M (1999) Activation of Rad53 kinase in response to DNA damage and its effect in modulating phosphorylation of the lagging strand DNA polymerase. *EMBO J* **18**: 6561–6572
- Poot M, Hoehn H, Runger TM, Martin GM (1992) Impaired S-phase transit of Werner syndrome cells expressed in lymphoblastoid cell lines. *Exp Cell Res* **202**: 267–273
- Sherman F (1991) Getting started with yeast. *Methods Enzymol* **194**: 3–21
- Shor E, Gangloff S, Wagner M, Weinstein J, Price G, Rothstein R (2002) Mutations in homologous recombination genes rescue top3 slow growth in *Saccharomyces cerevisiae*. *Genetics* **162**: 647–662
- Smith J, Rothstein R (1999) An allele of RFA1 suppresses RAD52-dependent double-strand break repair in *Saccharomyces cerevisiae*. *Genetics* **151**: 447–458
- Stewart E, Chapman CR, Al-Khodairy F, Carr AM, Enoch T (1997) rqh1+, a fission yeast gene related to the Bloom's and Werner's syndrome genes, is required for reversible S phase arrest. *EMBO J* **16**: 2682–2692
- Tong AH, Evangelista M, Parsons AB, Xu H, Bader GD, Page N, Robinson M, Raghibizadeh S, Hogue CW, Bussey H, Andrews B, Tyers M, Boone C (2001) Systematic genetic analysis with ordered arrays of yeast deletion mutants. *Science* **294**: 2364–2368
- Tong AH, Lesage G, Bader GD, Ding H, Xu H, Xin X, Young J, Berriz GF, Brost RL, Chang M, Chen Y, Cheng X, Chua G, Friesen H, Goldberg DS, Haynes J, Humphries C, He G, Hussein S, Ke L, Krogan N, Li Z, Levinson JN, Lu H, Menard P, Munyana C, Parsons AB, Ryan O, Tonikian R, Roberts T, Sdicu AM, Shapiro J, Sheikh B, Suter B, Wong SL, Zhang LV, Zhu H, Burd CG, Munro S, Sander C, Rine J, Greenblatt J, Peter M, Bretscher A, Bell G, Roth FP, Brown GW, Andrews B, Bussey H, Boone C (2004) Global mapping of the yeast genetic interaction network. *Science* **303**: 808–813
- Versini G, Comet I, Wu M, Hoopes L, Schwob E, Pasero P (2003) The yeast Sgs1 helicase is differentially required for genomic and ribosomal DNA replication. *EMBO J* **22**: 1939–1949
- Wallis JW, Chrebet G, Brodsky G, Rolfe M, Rothstein R (1989) A hyper-recombination mutation in *S. cerevisiae* identifies a novel eukaryotic topoisomerase. *Cell* **58**: 409–419
- Watt PM, Hickson ID, Borts RH, Louis EJ (1996) SGS1, a homologue of the Bloom's and Werner's syndrome genes, is required for maintenance of genome stability in *Saccharomyces cerevisiae*. *Genetics* **144**: 935–945
- Watt PM, Louis EJ, Borts RH, Hickson ID (1995) Sgs1: a eukaryotic homolog of *E. coli* RecQ that interacts with topoisomerase II *in vivo* and is required for faithful chromosome segregation. *Cell* **81**: 253–260
- Weinert TA, Kiser GL, Hartwell LH (1994) Mitotic checkpoint genes in budding yeast and the dependence of mitosis on DNA replication and repair. *Genes Dev* **8**: 652–665
- Winzeler EA, Shoemaker DD, Astromoff A, Liang H, Anderson K, Andre B, Bangham R, Benito R, Boeke JD, Bussey H, Chu AM, Connolly C, Davis K, Dietrich F, Dow SW, El Bakkoury M, Foury F, Friend SH, Gentalen E, Giaever G, Hegemann JH, Jones T, Laub M, Liao H, Liebundguth N, Lockhart DJ, Lucau-Danila A, Lussier M, M'Rabet N, Menard P, Mittmann M, Pai C, Rebischung C, Revuelta JL, Riles L, Roberts CJ, Ross-MacDonald P, Scherens B, Snyder M, Sookhai-Mahadeo S, Storms RK, Veronneau S, Veot M, Volckaert G, Ward TR, Wsocki R, Yen GS, Yu K, Zimmermann K, Philippson P, Johnston M, Davis RW (1999) Functional characterization of the *S. cerevisiae* genome by gene deletion and parallel analysis. *Science* **285**: 901–906
- Woods A, Sherwin T, Sasse R, MacRae TH, Baines AJ, Gull K (1989) Definition of individual components within the cytoskeleton of *Trypanosoma brucei* by a library of monoclonal antibodies. *J Cell Sci* **93**: 491–500
- Wu L, Davies SL, North PS, Goulaouic H, Riou JF, Turley H, Gatter KC, Hickson ID (2000) The Bloom's syndrome gene product interacts with topoisomerase III. *J Biol Chem* **275**: 9636–9644
- Wu L, Hickson ID (2003) The Bloom's syndrome helicase suppresses crossing over during homologous recombination. *Nature* **426**: 870–874
- Yamagata K, Kato J, Shimamoto A, Goto M, Furuichi Y, Ikeda H (1998) Bloom's and Werner's syndrome genes suppress hyperrecombination in yeast sgs1 mutant: implication for genomic instability in human diseases. *Proc Natl Acad Sci USA* **95**: 8733–8738
- Yin J, Soback A, Xu C, Meetei AR, Hoatlin M, Li L, Wang W (2005) BLAP75, an essential component of Bloom's syndrome protein complexes that maintain genome integrity. *EMBO J* **24**: 1465–1476
- Yu CE, Oshima J, Fu YH, Wijsman EM, Hisama F, Alisch R, Matthews S, Nakura J, Miki T, Ouais S, Martin GM, Mulligan J, Schellenberg GD (1996) Positional cloning of the Werner's syndrome gene. *Science* **272**: 258–262